Available online at www.sciencedirect.com
ScienceDirect
Nuclear Instruments and Methods in Physics Research B 260 (2007) 455–459
NIM B Beam Interactions with Materials & Atoms
www.elsevier.com/locate/nimb

Sidewall quality in proton beam writing

S.Y. Chiam *, J.A. van Kan, T. Osipowicz, C.N.B. Udalagama, F. Watt

Center for Ion Beam Applications, Department of Physics, National University of Singapore, 2, Science Drive 3, Singapore 117542, Singapore

Available online 14 February 2007

Abstract

Proton beam writing has been shown to allow the fabrication of high aspect ratio nanostructures at sub-100 nm dimension and with smooth and vertical sidewalls. For applications such as the fabrication of waveguides, sidewall smoothness is an important issue. We report results from investigations into side wall roughness measured directly with Atomic Force Microscopy. Structures were written in bulk poly(methylmethacrylate) (PMMA) with 2 MeV protons specifically to allow side access. We studied the effects of different scanning algorithms and also the variation of wall roughness with development time and ion penetration depth. Our results indicate that sidewall rms roughness of less than 7 nm is readily achievable. Multi-loop scanning and optimization of the scanning algorithm can lead to significant improvements in sidewall smoothness.

PACS: 07.78.+s; 85.40.Hp; 81.16.Nd; 81.15.Pq

Keywords: Proton beam writing; Cross sectional resist roughness; PMMA

1. Introduction

Proton beam writing (PBW) has been used successfully for the fabrication of high aspect ratio nanostructures with smooth and vertical sidewalls [1,2]. Applications of PBW include the fabrication of waveguides [3] and microfluidic structures [4]. For applications such as waveguides, sidewall roughness is also an important issue as it is a factor in determining the flux loss of an electromagnetic wave passing through the waveguide. Accurate statistical information about the sidewall morphologies of structures fabricated with PBW will allow the identification and optimization of the relevant parameters.

The presence of sidewall roughness in PBW can be attributed to several causes: (a) the dimensions of the proton beam spot (b) the scanning algorithm employed and the parameters used (c) variations in the beam intensity (d) development conditions, (e) unwanted external varying magnetic fields influencing the beam focusing and (f) stage vibrations, especially when PBW structures are fabricated with stage movement. Previous studies have been conducted on the sidewall morphology of PBW waveguides fabricated in SU8 [5], where waveguides have been fabricated using a combination of magnetic and stage scanning at the Center for Ion Beam Applications (CIBA). Direct roughness measurements on the sidewalls of these waveguides were carried out using atomic force microscopy (AFM).

Sidewall roughness is often assessed using Scanning Electron Microscopy (SEM). However, for non conducting polymers, SEM requires a conducting layer to be applied, possibly altering the surface morphology of the sidewall. Furthermore, to detect roughness at the nanometer level using SEM, high magnifications are necessary, increasing the risk of electron beam damage over the small area being imaged. Tapping mode AFM is ideal for the direct measurement of sidewall roughness, as it has nanometer scale vertical resolution and yields quantitative data such as root mean square roughness (R_{rms}), which is the standard deviation of height across the surface of a sample.

* Corresponding author. Fax: +65 67776126.
E-mail address: phycsy@nus.edu.sg (S.Y. Chiam).

0168-583X/$ - see front matter
doi:10.1016/j.nimb.2007.02.012

Here, we investigate the quality of side wall roughness in structures fabricated in bulk PMMA using proton beam writing, using different scanning algorithms (and including single loop and multi-loop). In addition we also present results on the variation of side wall smoothness as a function of development time and ion penetration depth.

2. Experimental

Structures were written with 2 MeV protons in pieces of bulk high molecular weight (several million) PMMA [6] cut from a larger sheet and then polished. The experiments were conducted using the PBW facility at CIBA [7,8]. In order to create structures where the sidewalls can be assessed with the AFM probe, the proton beam was scanned at the edge of a polished piece of PMMA such that only half of the rectangular scan area fell on the PMMA. When these samples are subsequently developed, a recessed "microstep" is created on the edge of the PMMA sample. These microsteps were typically 400 μm in length, with the sidewall recessed about 10–30 μm from the original surface of the PMMA. The depth of the step is determined by the penetration depth of 2 MeV protons into PMMA, which is about 60 μm from SRIM calculations [9]. An electron micrograph of one of these microsteps is shown on Fig. 1.

The microsteps were typically fabricated with a proton beam spot size of about 800 nm by 800 nm. Two different raster scan algorithms were used (Fig. 2). In one algorithm (L-algorithm), the fast scan axis was along the length of the microstep and thus parallel to the sidewall being studied. In the other algorithm (W-algorithm), the fast scan axis was across the width of the microstep and thus perpendicular to the sidewall being studied. The scan area was 400 μm long (4096 pixels) and 50 μm (512 pixels) wide. The size of a pixel is thus about 100 nm, significantly smaller that the beam spot size. Each pixel in the scan area is therefore swept several times by the beam, which is crucial for ensuring even dose distribution. Scanning of the proton beam is achieved using magnetic scan coils (OM 25) which are a part of the *Oxford Microbeams* scanning system.

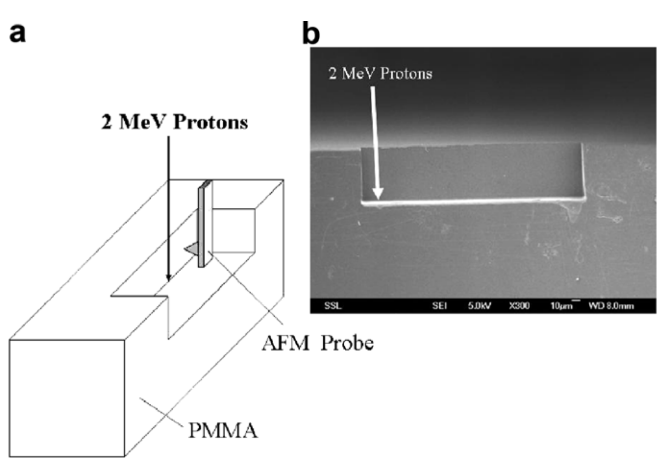

Fig. 1. (a) A schematic of the proton beam written "microstep" structure in PMMA. (b) Electron micrograph of a typical microstep fabricated in PMMA. The arrow indicates the direction of the 2 MeV proton beam used to fabricate the structure. Under the SEM, the sidewalls of these structures appear smooth even under high magnification, thus making the use of AFM necessary.

Typical irradiation doses for the microsteps were between 80 and 90 nC/mm^2. The beam currents and irradiation doses were determined using a calibrated RBS detector. It was assumed that the current was constant during the irradiation of each individual microstep, and thus the dwell time for each pixel in the microstep was kept constant.

For both scanning algorithms, both single loop and multi-loop scans were used. A loop is defined as the proton beam covering the entire scan area once. For single loop scans a typical pixel dwell time was about 200 μs. For multi-loop scans the pixel dwell time per loop was shortened to maintain the same total dwell time (and thus dose) per pixel.

Typical irradiation doses for the microsteps were between 80 and 90 nC/mm^2. Irradiation doses were determined using a calibrated RBS detector. It was assumed that the current was constant during the irradiation of each individual microstep, and thus the dwell time for each pixel in the microstep was kept constant.

After irradiation, the PMMA samples were developed using "GG Developer", a solution consisting of 60% diethylene glycol monobutyl ether, 20% morpholine, 5% ethanolamine and 15% water for between 10 and 15 min at 35–40 °C [6]. This was sufficient to remove the irradiated PMMA, exposing the proton beam written sidewalls.

The proton written sidewalls were then analyzed using tapping mode AFM (Digital Instruments Dimension™ 3000 SPM) using etched Si cantilever probes with a tip curvature of 5–10 nm. Typical scan areas were 5 μm by 5 μm or 20 μm by 20 μm. The cantilever was scanned perpendicular to beam direction for better sensitivity. The AFM images were then flattened using a low order polynomial fit, a standard procedure applied to remove image artifacts such as bow effects. Subsequently, R_{rms} values were extracted. Unless otherwise stated, the AFM data presented in this work were collected within 15 μm from the top edge of the microstep (i.e. within an ion penetration depth of 15 μm).

3. Results and discussion

Our results indicate that sidewall R_{rms} of less that 7 nm can be achieved readily when scan parameters are optimized. Fig. 3 shows typical AFM images taken over 5 μm by 5 μm areas of the sidewalls. The surface topology is dominated by striations parallel to the beam direction. These were present in all samples imaged with AFM for this work and were also present in the results reported by Sum et al. [5].

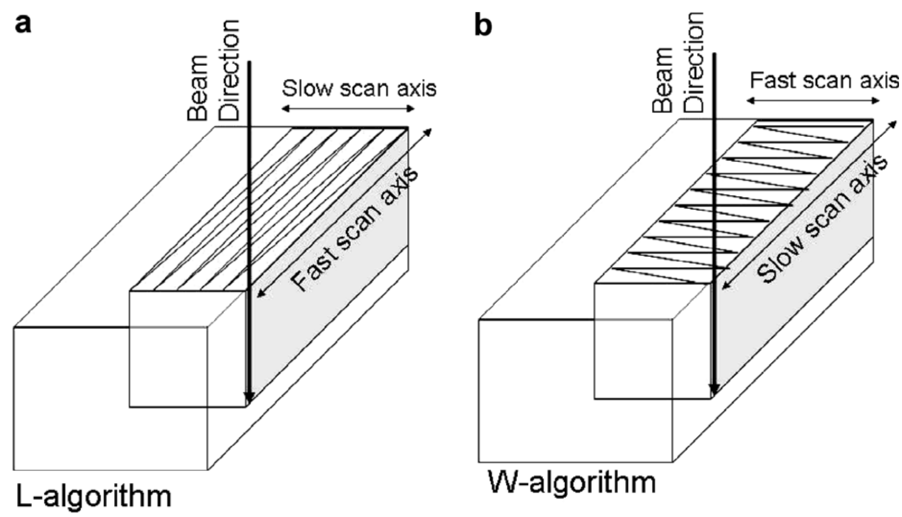

Fig. 2. Schematics of the two scanning algorithms used (a) L-algorithm with fast scan axis parallel to the length of the microstep. (b) W-algorithm with fast axis perpendicular to the length of the microstep. In these schematics the pitch of the raster scans, which is about 200 nm in our experiments, is greatly exaggerated.

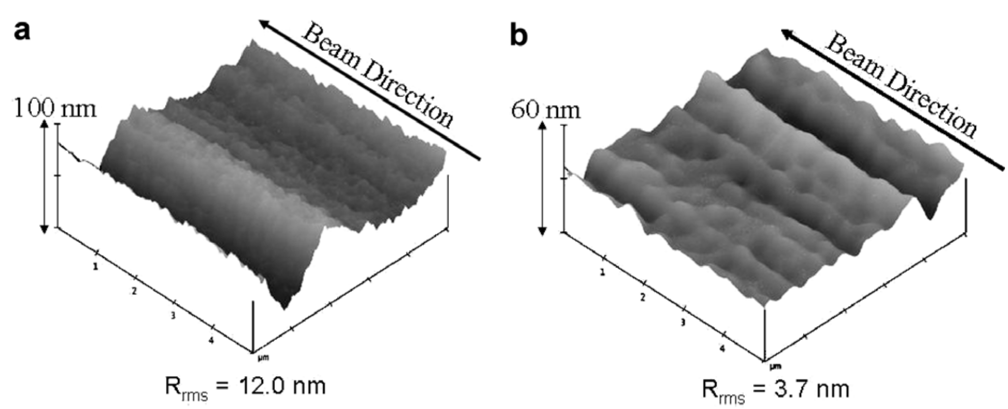

Fig. 3. Comparison of single (a) and multi-loop (b) scans. Both microsteps were fabricated using the L-algorithm, 3 scanning loops were used in (b).

3.1. Comparison of single and multi-loop scans

A comparison of the R_{rms} values for sidewalls fabricated using single-loop scans with those using multi-loop scans reveals that the latter can improve sidewall roughness considerably. In sidewalls fabricated using multi-loop scans the striations become visibly less pronounced, with the surface morphology displaying a more granular nature (See Fig. 3). As shown in Fig. 3, R_{rms} of 12 nm is observed in some cases using single loop scan. R_{rms} is significantly reduced using multi-loop scanning.

Multi-loop scans improved smoothness for both scanning algorithms (i.e. W-algorithm and L-algorithm). In both cases, multi-loop scans allowed the fabrication of sidewalls with R_{rms} significantly lower than 10 nm.

3.2. Comparison of scanning algorithms

Fig. 4 shows a comparison of AFM images for sidewalls fabricated using L-algorithm and W-algorithm, where 3 scan loops have be used for both algorithms. Visually, it can be seen that the striations produced by the W-algorithm are more regular in their amplitude and spacing. Using the L-algorithm, occasional deep striations are observed at more irregular intervals.

For a detailed comparison of the scanning algorithms, R_{rms} values were obtained from five AFM images for each scanning algorithm and an average computed. Each AFM image covered a 5 μm by 5 μm area of the sidewall. The results are shown in Table 1. The average R_{rms} obtained using L-algorithm (6.8 nm) is comparable to that obtained using W-algorithm (6.5 nm). However, the range of R_{rms} values is much larger for the L-algorithm then for the W-algorithm. This is consistent with the qualitative observation that the striations are less regular when the L-algorithm is used. This leads R_{rms} values to vary significantly across different scanning locations, depending on whether or not the scan area included a deeper striation. With W-algorithm, the more regular nature of the striations leads to consistent R_{rms} values.

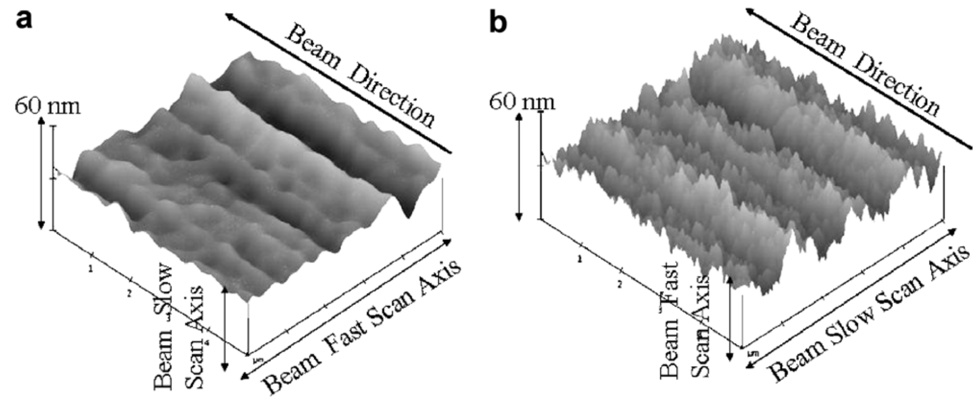

Fig. 4. Comparison scanning algorithms: (a) L-algorithm and (b) W algorithm. With the W-algorithm the striations are more regular in their depth and spacing.

Table 1
Comparison of scanning algorithms

	L-algorithm (nm)	W-algorithm (nm)
Average R_{rms}	6.8	6.5
Range (highest–lowest)	7.2	2.9

Table 2
Effects of resist development time

Development time	10 min (nm)	20 min (nm)
Average R_{rms}	6.5	7.1
Range (highest–lowest)	2.9	4.5

3.3. Effects of development time

At the nanometer level, sidewall roughness can be significantly affected by the development process. Studies on various electron beam resists have reported that sidewall roughness can be influenced by the developer molecule size [10], development time [11] and other processes like post development rinsing [12]. The relationship between development conditions and R_{rms} should thus be investigated. In this work, we investigated the relationship between development time and R_{rms}.

During the development process, it was found that a relatively short development time (10–15 min) was sufficient to remove the irradiated PMMA. This is probably because a large area (the top surface and an entire sidewall) of the irradiated region was in contact with the developer. A sample which had previously been developed for 10 min was placed in fresh developer for a further 10 min. The R_{rms} values before and after this second development are compared in Table 2. The microstep chosen for this comparison was irradiated using the W-algorithm with 3 scan loops. R_{rms} values were taken from five 5 μm by 5 μm areas and an average value computed. The results indicate a slight increase both in the average value and the spread of sidewall R_{rms} after the second development. Further work is necessary to study the influence of the development process on PBW sidewalls.

3.4. Effects of ion penetration depth

AFM results presented thus far have been collected from within the top quarter of the microsteps, where the protons have penetrated about 15 μm into the sample. For comparison, AFM data was also collected from the regions lower in the microstep, where the protons have penetrated deeper into the sample.

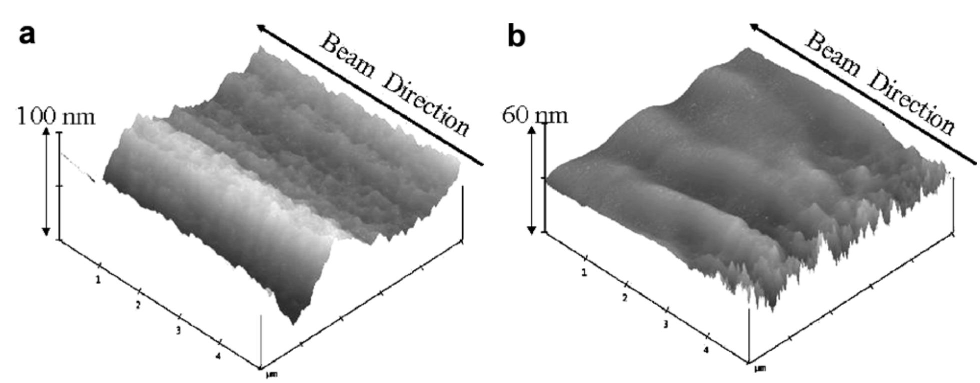

Fig. 5. Effects of ion penetration depth. AFM images were collected at an ion depth of 15 μm (a) and 45 μm (b). In (b) the effects of beam straggling are apparent. Striations become less pronounced and R_{rms} decreases.

Fig. 5 shows a comparison between AFM images collected at a depth of about 15 μm with one collected at a depth of about 45 μm. From the AFM image collected deeper in the sample, the effects of beam straggling can be directly observed. This leads the striations to become less pronounced and to a fall in the R_{rms} values. This effect indicates that the striations are indeed an artifact of the proton beam.

4. Discussion

Our present R_{rms} values of 6–7 nm are somewhat higher than values reported previously using the CIBA PBW facility. For example, van Kan et al. reported edge smoothness of less that 3 nm for a 30 nm wide line in 200 nm thick spin-coated PMMA [2], and Sum et al. reported a sidewall R_{rms} of 3.8 nm for PBW waveguides in SU8 using a combination of stage and magnetic scanning [5]. Even though our present experiments are not directly comparable with our previous work (which used different resist materials, structure geometry, etc.), it is likely that during our present experiments there was an additional factor (or factors) that contributed to an increase in side wall roughness.

Optimising structural integrity and side wall smoothness is an important goal in proton beam writing. There are many factors which can influence the side wall quality, and we have discussed these above. In our work, we have assumed the beam current to be stable during the irradiation of each microstep. Beam instability can play a major role in the deterioration of structural quality. It is well known that beam intensities and beam brightness from high voltage accelerators can vary with time. In our facility, these variations are mainly due to deterioration of ion source parameters, and this is particularly a problem in single ended accelerators with internal ion sources. There are stringent requirements for beam stability in proton beam writing, and any slight deterioration of beam quality, such as beam intensity fluctuations or energy changes, will undoubtedly lead to a deterioration of structural integrity and side wall smoothness.

We have observed that the use of multiple-loop scanning appreciably reduces the side wall roughness due to external factors. Even if we can minimize all the factors which reduce structural integrity, ultimately the sidewall roughness will be limited by inherent properties of the resist. AFM studies on the top surfaces of spin coated resist indicate R_{rms} values less than 0.5 nm [5]. However, it is not clear if such R_{rms} values can be achieved at the dissolution front of a resist due, for example, to the presence of polymer aggregates with diameters which are several tens of nanometers [13,14]. Further work is needed to better understand the properties of PBW sidewalls.

5. Conclusion

Our results indicate that R_{rms} of less than 7 nm can be readily achieved using the PBW facility at CIBA. The experimental evidence shows that multi-loop scanning improves R_{rms} significantly. The two scan algorithms we used achieve similar average values of R_{rms}, although there is a difference in spread of R_{rms} values. Near the end of range, R_{rms} values less then 3 nm are often recorded.

Acknowledgements

This work was supported by the Agency for Science, Technology and Research (ASTAR), under the grant no. R-144-000-130-112. The authors are also grateful to Dr. Andrew Bettiol and Ms. Fang Zhang for their constant help, encouragement and fruitful discussions.

References

[1] J.A. van Kan, A.A. Bettiol, K. Ansari, E.J. Teo, T.C. Sum, F. Watt, Int. J. Nanotechnol. 1 (4) (2004) 464.
[2] J.A. van Kan, A.A. Bettiol, F. Watt, Appl. Phys. Lett. 83 (8) (2003) 1629.
[3] A.A. Bettiol, S. Venugopal Rao, E.J. Teo, J.A. van Kan, Frank Watt, Appl. Phys. Lett. 88 (2006) 171106.
[4] P.G. Shao, J.A. Van Kan, L.P. Wang, K. Ansari, A. A Bettol, F. Watt, Appl. Phys. Lett. 88 (2006) 093515.
[5] T.C. Sum, A.A. Bettiol, H.L. Seng, J.A. van Kan, F. Watt, Appl. Phys. Lett. 85 (8) (2004) 1398.
[6] S.V. Springham, T. Osipowicz, J.L. Sanchez, L.H. Gan, F. Watt, Nucl. Instr. and Meth. B 130 (1997) 155.
[7] J.A. van Kan, A.A. Bettiol, F. Watt, in: Materials Research Society Symposium. Proceedings, 2003 p. 777.
[8] F. Watt, J.A. Van Kan, I. Rajta, A.A. Bettiol, T.F. Choo, M.B.H. Breese, T. Osipowicz, Nucl. Instr. and Meth. B 210 (2003) 14.
[9] J. Biersack, L.G. Haggmark, Nucl. Instr. and Meth. 174 (1980) 257.
[10] T. Yamaguchi, H. Namatsu, J. Vac. Sci. Technol. B 22 (3) (2004) 1037.
[11] S. Yasin, D.G. Hasko, M.N. Khalid, D.J. Weaver, H. Ahmed, J. Vac. Sci. Technol. B 22 (2) (2004) 574.
[12] S. Yasin, M.N. Khalid, D.G. Hasko, Jpn. J. Appl. Phys. Part 1 43 (10) (2004) 6984.
[13] T. Yamaguchi, K. Yamazaki, M. Nagase, H. Namatsu, Jpn. J. Appl. Phys. Part 1 42 (6B) (2003) 3755.
[14] T. Yamaguchi, H. Namatsu, M. Nagase, K. Yamazaki, K. Kurihara, Appl. Phys. Lett. 71 (1997) 2388.